High-Resolution Genetic Maps Identify Multiple Type 2 Diabetes Loci at Regulatory Hotspots in African Americans and Europeans

Winston Lau,[1] Toby Andrew,[2,3] and Nikolas Maniatis[1,3,*]

Interpretation of results from genome-wide association studies for T2D is challenging. Only very few loci have been replicated in African ancestry populations and the identification of the implicated functional genes remain largely undefined. We used genetic maps that capture detailed linkage disequilibrium information in European and African Americans and applied these to large T2D case-control samples in order to estimate locations for putative functional variants in both populations. Replicated T2D locations were tested for evidence of being regulatory hotspots using adipose expression. We validated a sample of our co-location intervals using next generation sequencing and functional annotation, including enhancers, transcription, and chromatin modifications. We identified 111 additional disease-susceptibility locations, 93 of which are cosmopolitan and 18 of which are European specific. We show that many previously known signals are also risk loci in African Americans. The majority of the disease locations appear to confer risk of T2D via the regulation of expression levels for a large number (266) of *cis*-regulated genes, the majority of which are not the nearest genes to the disease loci. Sequencing three cosmopolitan locations provided candidate functional variants that precisely co-locate with cell-specific chromatin domains and pancreatic islet enhancers. These variants have large effect sizes and are common across populations. Results show that disease-associated loci in different populations, gene expression, and cell-specific regulatory annotation can be effectively integrated by localizing these effects on high-resolution genetic maps. The *cis*-regulated genes provide insights into the complex molecular pathways involved and can be used as targets for sequencing and functional molecular studies.

Introduction

No disease with a genetic predisposition has been more intensely investigated than type 2 diabetes (T2D [MIM: 125853]), the world's most widespread and devastating metabolic disorder. Over the last 10 years, numerous consortia have undertaken to characterize the genetic causes of T2D through a very large number (>30) of genome-wide association studies (GWASs) and large-scale meta-analyses. Initially based on Europeans, the focus has now shifted to the replication of risk loci in additional ethnicities (trans-ethnic studies), motivated in part by the likely wider application of cosmopolitan variants for translational research, but also the desire for increasingly larger research sample sizes in order to try to boost study power.[1] But since T2D is really a group of diseases,[2] increased sample size should be met with skepticism unless accompanied by more detailed clinical phenotypes and strategies to minimize disease heterogeneity. Recent trans-ethnic meta-analysis of T2D for four populations (Europeans, East Asians, South Asians, and Mexican Americans) has identified 7 T2D loci,[3] in addition to the previously published list of 69 loci.[4] However, a large proportion of these 76 loci[3] do not show evidence for nominal association for the same "lead" SNP. Since the lead SNP is unlikely to be the causal variant, this low replication rate is a general problem for trans-ethnic studies.[5] The inability to account for genetic distance between neighboring SNPs and genetic heterogeneity (e.g., locus and allele heterogeneity and variation in LD between populations) are both potential thwarting factors in the endeavor to identify trans-ethnic disease loci.

On the other hand, the prevalence of T2D in African Americans (19%) at approximately twice that of European Americans (10%) and the existence of more genetic diversity in peoples of African ancestry, partly due to less extensive linkage disequilibrium (LD), also gives rise to a major opportunity for comparative fine-mapping studies.[3,6,7] This possibility was missed by a recent major trans-ethnic meta-analyses that unfortunately excluded African-Americans.[3] Here we seek to take advantage of this ancestry group by using a mapping approach to identify cosmopolitan T2D locations, which avoids the focus on lead SNPs. Instead we use high-resolution genetic maps to identify new cosmopolitan T2D susceptibility loci that are shared by both European and African American populations. Genetic distances from these maps accurately capture the genetic architecture of the relevant population and have been successfully used in gene-mapping studies for other common diseases.[8,9] We constructed genetic maps for each of these two populations and then used disease-associated location estimates on these maps as the basis for the precise co-localization and replication in both populations. We also analyzed all 76 previously known T2D loci[3] to obtain refined location estimates on the same genetic maps. Since an estimated 90% of variants with a functional role in

[1]Department of Genetics, Evolution and Environment, University College London, WC1E 6BT London, UK; [2]Department of Genomics of Common Disease, Imperial College London, W12 0NN London, UK
[3]These authors contributed equally to this work
*Correspondence: n.maniatis@ucl.ac.uk
http://dx.doi.org/10.1016/j.ajhg.2017.04.007.
© 2017

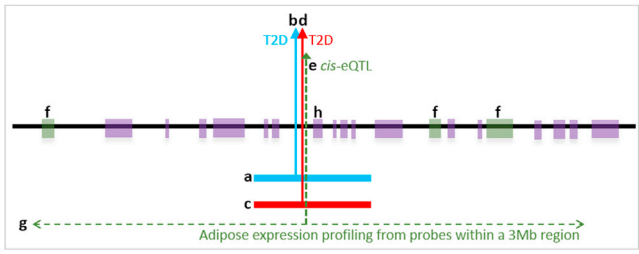

Figure 1. A Schematic Presentation of the Functional Genomic Study Design
Shown are the linkage disequilibrium unit (LDU) window of the European (EUR) genetic map (a); location of the causal variant for T2D estimated on the EUR map using a EUR GWAS (b); the corresponding African American (AA) LDU genetic map for the same region (c); location of the causal variant for T2D estimated on the AA map using an AA GWAS (d); location of the *cis*-eQTL (e) for the three associated *cis*-genes (f) that are implicated using adipose expression data (g) for probes from genes within ±1.5 Mb distance either side of the T2D locations (b and d). In this example the nearest gene (h) is not the implicated regulated gene.

complex traits such as T2D are likely to be non-coding and regulatory,[10] we assessed this scenario by exploiting publicly available subcutaneous adipose expression data. The hypothesis we tested is that T2D disease loci confer risk of disease by acting as expression quantitative trait loci (eQTL) that regulate the expression of neighboring (*cis*-) genes. To test this hypothesis (Figure 1), we used the same genetic maps to assess whether the location estimates for eQTL also precisely co-located with those mapped for T2D in this whole-genome analysis, thereby identifying potential *cis*-genes and pathways regulated by the disease loci. Finally, we performed fine mapping using targeted next generation sequencing (NGS) of the refined location estimates for one previously known locus (*TCFL72*) and two of the additional cosmopolitan loci from this study using independent case/control sample data, with the aim of identifying the candidate functional variants at the causal location estimates. These examples illustrate a way forward for the systematic identification of putative functional variants at these identified disease-associated eQTLs, coupled with the integration of functional annotation such as cell-specific chromatin domain modifications, enhancers, and transcription binding sites.

Subjects and Methods

Study Design

We analyzed two European (EUR) and one African American (AA) sample populations with a total of 5,800 T2D case subjects and 9,691 control subjects. The two independent EUR samples (SNP arrays for GWA and Metabochip) were obtained from the Wellcome Trust Case Control Consortium (WTCCC)[11,12] with a description of diagnostic criteria and sample matching provided in Supplemental Data. The AA GWA sample for a population of predominantly African ancestry was obtained from the National Institute of Diabetes and Digestive and Kidney Diseases (NIDDK).[13] Analyzing "one-SNP-at-a-time" ignores LD structure when testing for association with disease or gene expression. Here we use population-specific genetic maps, which provide (1) commensurability when making comparisons between different populations and SNP arrays; (2) the means to implement a multi-marker test of association;[14] (3) genetic distances between loci when testing for association with disease or adipose expression; and (4) precise location estimates on the genetic map for potential functional variants, since these estimates are more efficient than using physical maps.[15] We constructed two high-resolution genetic maps based upon HapMap data with genetic distances expressed in linkage disequilibrium units (LDU).[16] The EUR LDU map was used for analyses of the two EUR T2D datasets and the AA LDU map was used for the analysis of the AA T2D dataset. The autosomal genome (sex chromosomes were not included in the analyses) was divided into 4,800 non-overlapping analytical windows, each with a minimum distance of 10 LDU. In addition to windows being the same minimum size on the genetic map, each window also had to include a minimum of 30 SNPs. These criteria yielded an average genetic length of 11 LDU. The identical boundaries in kilobases (kb) for all 4,800 analytical windows were used for the AA dataset, but with longer average genetic length (16 LDU), reflecting a population history of greater antiquity with additional historical recombination events. All SNPs in each analytical window were simultaneously used to test for association with disease using a multi-marker LDU model.[14] The analysis returns one estimated location for a causal variant with the strongest signal, along with the association test p value for each window. Utilizing the genetic map in this way, the multi-marker test of association models the degree of regional LD when estimating the location of a putative causal variant on the genetic map. A schematic diagram of the functional genomic strategy used in the current study is provided in Figure 1. Strict criteria were used for the meta-analysis. Location estimates for genome-wide significant meta-analysis loci had to be nominally significant in both ancestry groups for the cosmopolitan loci and in both European samples for the European-specific loci. An interval criterion was used where location estimates from different datasets had to be within <100 kb of one another to qualify as a potential replication. Replicated loci had to pass a Bonferroni corrected meta-analysis p value threshold of 1×10^{-5}, based on the total number of genomic tests performed ($\alpha = 0.05/4{,}800$). We refer to the co-location interval (distance between location estimates) as the genomic region that most plausibly includes the functional variants that confer risk of T2D.

We conducted in silico functional gene expression analyses to assess whether the same T2D loci are also eQTL that regulate the expression of neighboring *cis*-genes using data generated by the MuTHER consortium.[17] Summary statistics for the probes and SNPs were available from the MuTHER website. Using adipose tissue mRNA expression probes as quantitative traits, we tested for *cis*-association at each disease locus by employing the same multi-locus LDU model, with potential regulated *cis*-genes defined to be within ±1.5 Mb distance either side of each replicated T2D causal location (Figure 1). We considered a disease locus to be a potential eQTL only if the estimated eQTL co-located to within 50 kb of the T2D location and passed Bonferroni correction for the total number of probes tested within ±1.5 Mb of each replicated disease locus. All LDU location estimates for both T2D and eQTL on the genetic map were converted back to kb B36 (NCBI36/hg18) for presentation purposes.

Finally, we conducted a NGS targeted re-sequencing experiment for three of the disease loci. Next generation sequencing was

conducted using the Agilent SureSelect^{XT2} capture kit following manufacturer protocol guidelines for 100 ng of DNA. Blood DNA samples were sequenced for a total of 94 unrelated European individuals with T2D and 94 unaffected controls 1:1 matched for age, BMI, and sex. Case subjects with a family history of T2D (selection and diagnosis criteria described elsewhere)[18] and control subjects were selected from families originally collected for an obesity (MIM: 601665) study without a history of T2D.[19] Additional method details are provided in the Supplemental Data.

Results

Additional Loci for T2D

Tables 1 and 2 present the results for the 111 additional loci associated with T2D. Of the 111 loci, 93 provide evidence of being cosmopolitan (signals 1–93, Table 1), since these loci replicate for both EUR and AA samples, while 18 loci appear to be European specific (94–111, Table 2), with replication in European samples only. The distances between T2D location estimates for the majority of the 111 loci were narrow (<50 kb apart). Estimation of average pairwise D-prime (D′) for all HapMap SNPs found within all the identified 111 disease location intervals (ranging from 0 to <100 kb) is D′ = 0.86 in EUR and D′ = 0.78 in AA, which reflect the importance of using a genetic map in LDU distances for localization and the <100 kb interval as a criterion for replication. For the majority of the cosmopolitan loci (signals 6–80, Table 1), the Metabochip array was not informative due to the very low SNP coverage in many regions (symbol "–" in Table 1). Some signals for Metabochip passed the minimal number of SNPs (>30 per window) but did not provide significant evidence of association ("NS" in Table 1) due to the uneven genomic coverage of SNPs on the customized Metabochip design.[12] For this reason, there were only 13 cosmopolitan loci (signals 81–93, Table 1) that provided replicated evidence for AA and Metabochip European samples.

For the 111 additional T2D loci, half of the location estimates are intragenic and half are intergenic. For the latter, we follow the convention of labeling the disease loci using the nearest gene symbol (within 100 kb from the T2D location). The in silico expression analyses, however, indicate which *cis*-genes are regulated and therefore functionally implicated by the identified T2D loci. Two-thirds (71/111) of the disease loci also show strong evidence of being eQTLs using our stringent criteria but the remaining one-third may well reflect that these replicated loci could be eQTLs for a T2D-relevant tissue other than subcutaneous adipose. The 71 eQTL signals regulate the expression of a conservatively estimated total of 183 *cis*-genes (Tables 1 and 2), the majority of which are not genes that are the nearest to the disease locus. Indeed, further investigation of the 183 *cis*-genes substantiates quantitatively what has previously been suspected: namely, that the physical kb distance of the eQTL to the *nearest* gene (Figure 1) is entirely unrelated ($p > 0.05$) to the distance between the same eQTL and the actual (*cis*-associated) *functional* gene (see Figure S1). This result demonstrates that the assumption that the nearest gene is also the most likely candidate functional gene is not justified. Further analysis of the 183 *cis*-genes also showed that the distance between the eQTL and the T2D location estimates is not biased by the distance between the T2D sample location estimates within the <100 kb interval (see Figure S2).

Interestingly, approximately 40% of the eQTL signals observed in this study have at least one *cis*-gene whose expression (in adipose or liver) is also strongly associated with BMI in morbidly obese individuals.[20] We also show that a number of the identified T2D loci also regulate the expression levels of nuclear-encoded mitochondrial genes. For example, many *cis*-genes implicate T2D through the regulation of the molecular functions of fatty acid metabolism (*PCCA* [MIM: 232000], *ACAD11* [MIM: 614288], signals 66 and 99, respectively), glycerophospholipid metabolism (*PISD* [MIM: 612770], *GPAM* [MIM: 602395], signals 80 and 117), pyruvate metabolism (*PDHA2* [MIM: 179061], *HAGH* [MIM: 138760], signals 26/27 and 68), mitochondrial transcription and translation (*MTERFD3* [MIM: 616929], *LACTB* [MIM: 608440], *TRMT11* [MIM: 609752], signals 61, 90, 105), and mitochondrial protein transport (*GFER* [MIM: 600924], signal 68). The *cis*-genes *PDHA2* and *PCCA* (signals 26/27 and 66, respectively) directly implicate the genetic dysregulation of Krebs cycle function as a risk factor for T2D.

To further characterize the observed T2D and associated eQTL location estimates in relation to potential functional variants, three of the cosmopolitan loci were targeted for sequencing using an independent sample of Europeans. Figure 2 presents an example of a regulatory intergenic hotspot near *ACTL7B* (MIM: 604304) on chromosome 9q31.3 (signal 46, Table 1). The two genetic maps (y axis in LDU) for AA and EUR are plotted against the physical genomic region (x axis in kb), with each data point representing a HapMap SNP from which the genetic LDU maps were inferred (Figure 2B). Cumulative LDU plots the nonlinear relationship between physical distance and the underlying LD, which is typically a "Block-Step" structure. Blocks of LD (SNPs with the same LDU location) represent areas of conserved LD and low haplotype diversity, and steps (increasing LDU distances) define LD breakdown, primarily caused by recombination, since crossover profiles agree precisely with the corresponding LDU steps.[16] The maps show numerous short blocks across the entire region with total LDU length being greater for AA (greater LD breakdown) than the EUR population. The functional location estimates A and E (13 kb apart) indicated by the vertical solid line arrows are associated with T2D in AA and EUR samples, respectively. The dotted lines, in close proximity to the T2D locations (<30 kb), represent the location of eQTLs that regulate the expression of *KLF4* (MIM: 602253) and *EPB41L4B* (MIM: 610340) in subcutaneous adipose (nine genes reside between the two illustrated, but for clarity only the *cis*-genes regulated by the T2D-associated eQTL are plotted). *KLF4* and *EPB41L4B*

Table 1. Identified Cosmopolitan T2D Susceptibility Loci and Their Regulatory Role of Neighboring Gene Expression

Signal	Chr.	Meta p Value	Distance between Locations[a]	T2D Location GWAS-E[b]	T2D Location GWAS-A[c]	T2D Location metabo-E[d]	Nearest Gene to T2D Locations[e]	No. of *cis*-Genes[f]	eQTL-Associated *cis*-Genes[g]	eQTL Distance from T2D[h]
1	4p	1.73×10^{-56}	1	44,797	44,857	44,858	–	0	–	–
2	6q	5.28×10^{-10}	4	72,479	72,509	72,505	–	1	*FAM135A*	1
3	13q	2.14×10^{-35}	28	109,848	109,805	109,833	*COL4A2**	1	*ANKRD10*	20
4	17q	2.80×10^{-12}	7	65,769	65,762	65,769	*KCNJ2**	1	*MAP2K6*	37
5	20q	1.83×10^{-6}	77	44,104	44,181	44,104	*SLC12A5**, *CD40*+*	2	*CD40, CDH22*	17
6	1p	2.48×10^{-6}	41	82,826	82,867	–	–	1	*LPHN2**	8
7	1p	5.20×10^{-7}	73	84,451	84,524	–	*PRKACB*+*, *SAMD13*+*	3	*PRKACB, SAMD13, C1orf52*	6
8	1p	1.79×10^{-11}	94	106,441	106,535	–	–	1	*PRMT6*	3
9	1q	5.03×10^{-14}	8	207,662	207,670	–	*MIR205HG**	0	–	–
10	1q	3.40×10^{-9}	3	232,337	232,340	–	*SLC35F3**	0	–	–
11	1q	1.07×10^{-7}	52	234,896	234,948	–	*ACTN2**	3	*TBCE**, *B3GALNT2, ARID4B*	23
12	1q	6.33×10^{-7}	49	243,993	244,042	–	*SMYD3**	0	–	–
13	2p	4.57×10^{-7}	95	12,139	12,044	–	*MIR3681HG**	0	–	–
14	2p	2.62×10^{-15}	89	45,025	44,936	–	*SIX3**, *CAMKMT*	3	*PRKCE**, *DYNC2LI1, ABCG8*	27
15	2q	2.61×10^{-9}	89	139,530	139,527	–	–	0	–	–
16	3p	4.05×10^{-7}	42	7,503	7,461	–	*GRM7**	1	*RAD18*	17
17	3p	1.20×10^{-10}	0	38,370	38,369	NS	*XYLB**	0	–	–
18	3p	5.10×10^{-11}	95	41,078	41,173	NS	*CTNNB1*	2	*CTNNB1**, *ZNF621*	1
19	3p	4.22×10^{-23}	13	47,556	47,569	NS	*CSPG5*	4	*IP6K2 (IHPK2)**, *KIF9, TESSP5, P4HTM*	3
20	3p	8.39×10^{-6}	20	54,986	54,965	–	*CACNA2D3**	0	–	–
21	3p	1.13×10^{-13}	59	67,827	67,768	–	*SUCLG2*	0	–	–
22	3p	6.67×10^{-10}	9	87,317	87,327	NS	*CHMP2B*	0	–	–
23	3q	7.80×10^{-6}	18	122,056	122,038	–	*BC032918*	2	*CD86**, *ILDR1*	4
24	3q	5.39×10^{-8}	49	184,743	184,694	–	*KLHL6**	3	*AP2M1, ABCF3, MAGEF1*	0
25	4q	1.87×10^{-11}	24	53,132	53,108	NS	*USP46*+*	1	*USP46*	2
26	4q	2.68×10^{-7}	6	92,162	92,168	–	*CCSER1**	2	*HSD17B13, PDHA2*	0
27	4q	5.24×10^{-13}	56	96,319	96,376	–	*UNC5C**	1	*PDHA2*	2
28	4q	4.02×10^{-13}	3	102,095	102,098	–	*PPP3CA*	0	–	–
29	4q	1.50×10^{-6}	74	148,449	148,375	>100 kb	–	1	*EDNRA*	1
30	5q	8.84×10^{-6}	44	52,127	52,083	–	*PELO**	1	*ITGA1*	20
31	5q	1.56×10^{-8}	14	59,263	59,277	–	*PDE4D*+*	1	*PDE4D**	38
32	5q	2.81×10^{-6}	77	97,282	97,359	–	–	0	–	–
33	6p	1.00×10^{-7}	86	40,514	40,429	–	*LRFN2**, *BC132805**	2	*KCNK5, UNC5CL**	0
34	6p	1.30×10^{-15}	72	44,790	44,718	–	*BX647715*	1	*PTK7*	4
35	6q	3.04×10^{-7}	5	168,842	168,837	–	*SMOC2*	3	*MLLT4**, *CCR6, C6orf122*	1

(*Continued on next page*)

Table 1. ***Continued***

Signal	Chr.	Meta p Value	Distance between Locations[a]	T2D Location GWAS-E[b]	T2D Location GWAS-A[c]	T2D Location metabo-E[d]	Nearest Gene to T2D Locations[e]	No. of *cis*-Genes[f]	eQTL-Associated *cis*-Genes[g]	eQTL Distance from T2D[h]	
36	7p	6.93×10^{-8}	85	24,390	24,305	–	*NPY*	2	*CCDC126, OSBPL3*	35	
37	7p	1.49×10^{-8}	4	35,510	35,514	–	*HERPUD2*	1	*AAA1*	34	
38	7p	5.97×10^{-6}	75	37,471	37,396	–	*ELMO1**+	2	*ELMO1, GPR141*	30	
39	7q	4.00×10^{-6}	77	82,225	82,149	–	*PCLO**	1	*HGF**	26	
40	7q	4.78×10^{-12}	62	132,516	132,454	–	*CHCHD3*	0	–		–
41	7q	1.30×10^{-9}	73	133,716	133,789	–	*SLC35B4, AKR1B1**	0	–		–
42	7q	4.44×10^{-10}	14	134,336	134,322	–	*AGBL3**	1	*TMEM140**	0	
43	7q	6.98×10^{-14}	75	141,873	141,798	–	*TCRBV20S1**, *TCRB**	4	*FAM131B**, *ZYX, OR2A25, OR2F1*	0	
44	8p	4.81×10^{-8}	93	14,339	14,246	–	*SGCZ**	2	*C8orf79, TUSC3*	11	
45	8q	7.00×10^{-8}	87	70,416	70,503	–	*SULF1*	1	*PRDM14*	46	
46	9q	6.46×10^{-8}	13	110,613	110,626	NS	*ACTL7B*	2	*EPB41L4B**, *KLF4*	29	
47	9q	8.64×10^{-7}	19	132,799	132,781	–	*FIBCD1**	4	*ABL1**, *AIF1L, RAPGEF1** *PRDM12*	23	
48	10q	5.13×10^{-10}	11	44,467	44,456	>100 kb	–	1	*ZNF22**	32	
49	10q	1.28×10^{-6}	8	57,261	57,268	–	–	1	*CDC2*	0	
50	10q	9.29×10^{-9}	0	65,408	65,408	NS	*CR622643*	0	–		–
51	10q	8.37×10^{-11}	66	77,817	77,883	–	*C10orf11**+	2	*C10orf11, DUPD1*	1	
52	11p	4.29×10^{-9}	5	22,257	22,262	–	*ANO5**	0	–		–
53	11p	5.53×10^{-13}	88	32,453	32,364	–	*WT1**+	4	*PRRG4**, *FBXO3**, *ELP4, WT1*	14	
54	11q	4.12×10^{-8}	0	57,558	57,558	NS	*OR9Q1**	1	*MPEG1*	33	
55	11q	1.11×10^{-9}	21	59,295	59,315	–	*STX3**	0	–		–
56	12p	1.40×10^{-7}	31	25,404	25,373	–	*KRAS*	1	*SSPN*	0	
57	12p	8.75×10^{-7}	6	29,568	29,574	–	*TMTC1**	0	–		–
58	12q	3.45×10^{-6}	91	57,035	57,127	NS	–	2	*SLC26A10, MBD6*	1	
59	12q	8.78×10^{-6}	34	61,602	61,636	–	*PPM1H**	0	–		–
60	12q	2.45×10^{-6}	62	98,425	98,363	–	*ANKS1B**	0	–		–
61	12q	1.45×10^{-6}	22	104,931	104,909	–	*NUAK1*	1	*MTERFD3*	0	
62	13q	2.09×10^{-7}	85	26,479	26,564	–	*USP12**	0	–		–
63	13q	8.19×10^{-6}	40	47,133	47,173	–	–	0	–		–
64	13q	7.16×10^{-14}	13	65,393	65,380	–	*MIR548X2*	0	–		–
65	13q	1.10×10^{-14}	82	66,885	66,803	–	–	0	–		–
66	13q	5.74×10^{-7}	44	101,207	101,251	–	*FGF14**+	3	*TMTC4, PCCA, FGF14*	0	
67	15q	1.13×10^{-6}	16	45,938	45,954	–	*LINC01494*	0	–		–
68	16p	2.90×10^{-10}	80	1,700	1,781	–	*MAPK8IP3, IGFALS*	7	*HAGH**, *PGP**, *TPSAB1**, *FAHD1, GFER, GNPTG, PRR25*	0	
69	16p	2.24×10^{-6}	32	12,605	12,636	–	*SNX29*	3	*CLEC16A**, *SOCS1, LITAF*	10	
70	16q	1.75×10^{-26}	4	70,999	70,995	>100 kb	*AK055364*	1	*HYDIN*	2	

(*Continued on next page*)

Table 1. *Continued*

Signal	Chr.	Meta p Value	Distance between Locations[a]	T2D Location GWAS-E[b]	T2D Location GWAS-A[c]	T2D Location metabo-E[d]	Nearest Gene to T2D Locations[e]	No. of *cis*-Genes[f]	eQTL-Associated *cis*-Genes[g]	eQTL Distance from T2D[h]
71	16q	1.03×10^{-11}	20	77,036	77,016	–	*WWOX**	0	–	–
72	16q	5.52×10^{-19}	29	78,435	78,406	–	*LOC101928248*	2	*MAF**, *WWOX*	11
73	17q	4.15×10^{-7}	47	34,640	34,593	>100 kb	*STAC2*, *CACNB1**	4	*PLXDC1, CRKRS, ZPBP2, KRT222*	6
74	18q	9.58×10^{-10}	0	36,270	36,271	–	–	0	–	–
75	18q	6.84×10^{-6}	72	74,880	74,809	–	*SALL3*	0	–	–
76	21q	3.09×10^{-9}	30	20,521	20,490	–	*DYRK1A*	0	–	–
77	21q	9.56×10^{-8}	61	27,738	27,677	–	*MIR5009*	0	–	–
78	21q	1.35×10^{-10}	39	34,148	34,109	–	*ITSN**	2	*C21orf66, TCP10L*	0
79	21q	1.53×10^{-6}	1	37,635	37,633	–	*DYRK1A*	1	*KCNJ6*	0
80	22q	7.29×10^{-9}	0	31,376	31,376	–	*SYN3**	1	*PISD*	12
81	2p	6.46×10^{-6}	7	NS	21,294	21,301	–	1	*SDC1*	33
82	2p	5.02×10^{-9}	0	>100 kb	26,774	26,774	*KCNK3*	6	*OTOF**, *GAREM2, CCDC121, ASXL2, DNMT3A, CENPA*	3
83	2q	1.02×10^{-11}	1	>100 kb	135,313	135,313	*ACMSD**	0	–	–
84	2q	2.25×10^{-11}	0	NS	203,732	203,732	*NBEAL1*	0	–	–
85	4q	2.77×10^{-9}	8	>100 kb	103,404	103,395	*SLC39A8**+	1	*SLC39A8*	0
86	6p	2.09×10^{-13}	60	NS	28,525	28,586	*ZSCAN23, PX6*	8	*ZKSCAN3, PGBD1**, *MAS1L, OR2W1, OR11A1, HLA-F, IFITM4P, ZNF184*	6
87	8p	1.54×10^{-18}	44	>100 kb	18,194	18,238	*NAT1, NAT2*	3	*PDGFRL**, *CSGALNACT1, PCM1*	1
88	11p	1.86×10^{-20}	86	>100 kb	8,508	8,594	*STK33**, *TRIM66**	0	–	–
89	12q	4.10×10^{-16}	44	>100 kb	48,574	48,618	*FAIM2**+	1	*FAIM2*	10
90	15q	1.93×10^{-7}	77	NS	61,133	61,210	*TPM1**+, *LACTB**+	9	*TPM1, RPS27L**, *DAPK2**, *SNX1, LACTB, APH1B, HERC1, FAM96A, VPS13C*	1
91	17q	2.02×10^{-6}	86	>100 kb	44,633	44,548	*GNGT2**+, *B4GALNT2*	3	*GNGT2, SAMD14**, *HOXB3**	19
92	17q	3.95×10^{-8}	85	>100 kb	60,951	60,866	*AXIN2**+	1	*AXIN2*	38
93	20p	1.90×10^{-19}	31	>100 kb	25,718	25,687	*FAM182B**	0	–	–

[a]T2D-associated intervals in kb (<100) that harbor T2D susceptibility loci in both populations; the minimum distance is provided for signals 1–5
[b]Location estimates for the European (E) GWASS
[c]Location estimates for the African American (A) GWASS
[d]Location estimates for the Metaboship European (E) samples; signals with low SNP coverage (indicated by "–") were not meta-analyzed
[e]Genes with asterisk (*) denote the intragenic localization and genes with plus sign (+) indicate self-regulatory
[f]Number of *cis*-genes regulated by the eQTL
[g]List of *cis*-genes associated with eQTLs that co-located within <50 kb of the T2D locations; *cis*-genes with asterisk (*) have previously shown evidence of association between body mass index in morbidly obese and adipose/liver expression profiles[20]
[h]Distance in kb (<50) between eQTL and T2D locations; the minimum is given when more than one *cis*-gene is implicated

are 1.3 Mb downstream and 350 kb upstream, respectively. Targeted next-generation re-sequencing of the 39 kb region centered on these A and E locations shows evidence of association between T2D and variants, which coincide with the estimates for the T2D-associated eQTL (summary statistics of the NGS SNPs are provided in Figure 2A). Although only nominally significant ($p < 0.05$) due to small sample size (94 case subjects and 94 control subjects), these common variants both confirm the expected location estimate and account for a relatively large risk of

Table 2. Identified European-Specific T2D Susceptibility Loci and Their Regulatory Role of Neighboring Gene Expression

Signal	Chr.	Meta p Value	Distance of T2D Locations[a]	T2D Location GWAS-E[b]	T2D Location GWAS-A[c]	T2D Location metabo-E[d]	Nearest Gene to T2D Locations[e]	No. of *cis*-Genes[f]	eQTL Associated *cis*-Genes[g]	eQTL Distance from T2D[h]
94	1p	2.02×10^{-7}	3	25,879	NS	25,876	*MAN1C1**	2	*DHDDS, C1orf172*	0
95	1q	6.94×10^{-12}	21	228,322	NS	228,344	*GALNT2**	0	–	–
96	2p	4.11×10^{-34}	34	605	NS	639	*TMEM18*	0	–	–
97	2p	1.18×10^{-7}	46	40,320	>100 kb	40,274	*SLC8A1-AS1**	4	*THUMPD2, TMEM178, MORN2, DHX57*	0
98	3p	1.03×10^{-9}	5	53,518	NS	53,513	*CACNA1D**	0	–	–
99	3q	9.35×10^{-7}	7	133,919	NS	133,912	*ACAD11*+*	8	*ACAD11, SLC02A1, RYK, NPHP3, ACKR4, SRPRB, CDV3, RAB6B*	0
100	4q	1.86×10^{-22}	66	104,224	>100 kb	104,157	*BDH2, NHEDC1*	0	–	–
101	5q	2.62×10^{-9}	12	76,449	NS	76,461	*ZBED3*	1	*PDE8B**	15
102	6p	2.64×10^{-24}	13	29,662	NS	29,674	*GABBR1*	7	*GNL1*, TRIM10, TRIM27, DDR1, TRIM40, TRIM15, OR10C1*	9
103	6p	1.46×10^{-28}	6	31,709	>100 kb	31,704	*BAT2, AIF1*	14	*AIF1*, TRIM39*, AGER, BAT4, CCHCR1, DOM3Z, EHMT2, HLA-DMB, HLA-DPA1, HSPA1B, LST1, TRIM10, NOTCH4, HLA-DRA*	0
104	6q	6.29×10^{-56}	0	118,801	>100 kb	118,801	*SLC35F1*	0	–	–
105	6q	4.23×10^{-17}	37	127,581	NS	127,544	*RSPO3*+*	2	*RSPO3, TRMT11*	1
106	10q	3.39×10^{-24}	40	104,790	>100 kb	104,830	*CNNM2**	0	–	–
107	11p	2.50×10^{-6}	1	43,836	NS	43,836	*HSD17B12*	1	*HSD17B12*	1
108	11q	6.39×10^{-6}	21	65,337	>100 kb	65,357	*OVOL1, SNX32*+*	4	*SNX32, MAJIN*, SNX15, EFEMP2*	9
109	12q	6.16×10^{-6}	4	54,905	>100 kb	54,909	*OBFC2B*+*	4	*OBFC2B, RGL1*, RPS26, STAT2*	0
110	12q	4.66×10^{-8}	3	111,476	>100 kb	111,473	*PTPN11*	4	*ERP29, TMEM116, MAPKAPK5, NAP1*	20
111	17q	3.05×10^{-9}	51	25,003	>100 kb	25,054	*SSH2**	1	*CORO6*	9

[a]T2D associated intervals in kb (<100) that harbor T2D susceptibility loci in two European populations
[b]T2D location estimates for the European (E) GWAS
[c]The African American (A) GWAS yielded either significant but distant locations from the European T2D location (>100 kb) or not significant (NS) estimates
[d]Location estimates for the Metaboship European (E) samples that were within <100 kb of the GWAS-E location
[e]Genes with asterisk (*) denote the intragenic localization and genes with plus sign (+) indicate self-regulatory genes
[f]Number of *cis*-genes regulated by the eQTLs
[g]List of *cis*-genes associated with eQTLs that co-located within <50 kb of the T2D locus, *cis*-genes with asterisk (*) have previously shown evidence of association between body mass index for morbidly obese and adipose/liver expression profiles[20]
[h]Distance in kb (<50) between eQTL and T2D locations, the minimum is given when more than one *cis*-gene is implicated

disease (odds ratio [OR] of 2.0–2.4), with the risk allele frequencies (RAF) being similar in a number of human populations from the 1000 Genomes Project. Examination of the epigenetic chromatin marks from trimethylation of histone H3 at lysine 4 (H3K4me3) and acetylation of histone H3 at lysine 27 (H3K27ac), which highlight regulatory elements such as active promoters and enhancers,[21] has previously been shown to overlap with T2D loci,[22] but such marks are often cell type specific.[23] Figure 2C plots the −log10 p values of the chromatin profiles, demonstrating that T2D causal locations also co-localize with chromatin domains for $CD14^+$ monocytes and adipose nuclei. The most intense chromatin peaks were observed in $CD14^+$ monocytes at the precise eQTL location for *KLF4* and at rs60388922 and rs72756001 SNPs, which reside within the E and A T2D interval. Hence both of these SNPs are good causal candidate variants.

Figure 3 presents the regulatory potassium channel, subfamily k, member 3 (*KCNK3* [MIM: 603220]) locus (signal 82, Table 1) on chromosome 2p23.3 with identical

A

		Allele		Summary statistics			RAF in other human populations				
NGS SNPs	kb (B36)	risk	other	OR	*P*	RAF	EUR	AA	EAS	SAS	AMR
rs13285616	110597	A	G	2.04	2.4E-02	0.908	0.860	0.992	0.997	0.914	0.922
rs60388922	110619	G	T	2.09	3.7E-02	0.136	0.083	0.025	0.174	0.081	0.035
rs72756001	110624	A	G	2.40	3.1E-02	0.109	0.089	0.074	0.163	0.133	0.197
rs10979533	110628	G	T	2.21	4.2E-02	0.946	0.926	0.877	0.997	0.860	0.935
rs12380226	110629	T	C	2.21	4.2E-02	0.946	0.926	0.877	0.997	0.860	0.935

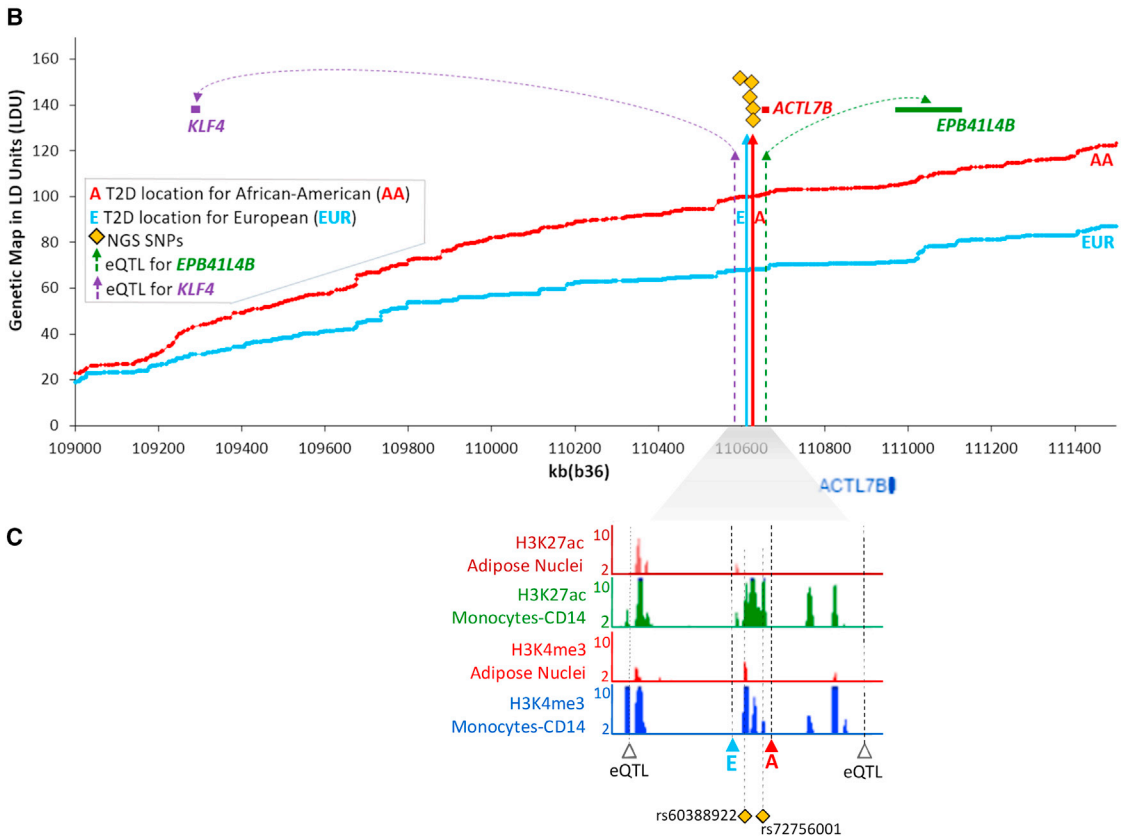

Figure 2. Candidate Causal Variants at T2D Locations in the *ACTL7B* Region and Their Regulatory Role
(A) Identified T2D-associated SNPs using targeted next generation sequencing (NGS) of the functional location estimates on the LDU genetic maps and their risk allele frequency (RAF) in Europeans (EUR), African Americans (AA), East Asian (EAS), South Asian (SAS), and Mexican Americans (AMR).
(B) The two LDU genetic maps (y axis in LDU) for AA and EUR are plotted against the physical genomic region (x axis in kb). Vertical solid arrows represent the functional location estimates A and E that are associated with T2D in AA and EUR samples, respectively. The dotted line arrows are the locations of eQTLs.
(C) −log10 p values of cell type-specific chromatin profiles are plotted against the kb map. T2D, eQTL, and NGS SNP locations overlap with the co-ordinates of the chromatin peaks.

location estimates for both AA and EUR samples (Figure 3B). Despite the disease locus residing within *KCNK3*, expression analyses indicate that this locus may not be functionally related to this gene, but instead is a *cis*-eQTL that regulates the distant genes *DNMT3A* (MIM: 602769), *ASXL2* (MIM: 612991), *GAREM2*, *OTOF* (MIM: 603681), *CENPA* (MIM: 117139), and *CCDC121*, with *DNMT3A* and *CCDC121* being 1.5 Mb and 896 kb away from the eQTL, respectively. This is a gene-rich region (57 genes in total), but for clarity only the six identified *cis*-genes have been plotted. Figure 3A presents summary statistics for the variants associated with T2D for a 42 kb targeted re-sequence region. These associated variants (p value < 0.05) coincide with the promoter region of *KCNK3*, 11 kb upstream of the T2D location estimate and account for a high risk of disease (OR = 3.5–4.8). The RAF are approximately 0.05 and the results show that these variants are indeed cosmopolitan, since they are common not only in EUR and AA but also in other human populations (e.g., East and South Asians and Mexican Americans). Using information from the human pancreatic islet regulome,[22] where sequences targeted by islet transcription factors highlight active enhancers, we observed that the identified T2D location resides within a cluster of such active enhancers. The transcription factor FOXA2-bound sites are also plotted within the kb boundaries of the active enhancer cluster. Chromatin peaks also overlap with the regulatory T2D and eQTL locations for pancreas and liver

A

		Allele		Summary statistics			RAF in other human populations				
NGS SNPs ◆	kb (B36)	risk	other	OR	*P*	RAF	EUR	AA	EAS	SAS	AMR
rs78489206	26751	A	G	4.73	3.1E-02	0.049	0.047	0.025	0.053	0.112	0.013
rs77786658	26753	A	G	4.85	2.8E-02	0.051	0.047	0.025	0.053	0.111	0.013
rs6707973	26755	G	A	3.51	4.6E-02	0.054	0.050	0.443	0.057	0.117	0.059
rs59284336	26760	T	C	4.73	3.1E-02	0.049	0.047	0.033	0.058	0.099	0.013
rs113076024	26763	A	G	4.79	2.9E-02	0.050	0.047	0.033	0.057	0.087	0.013

B

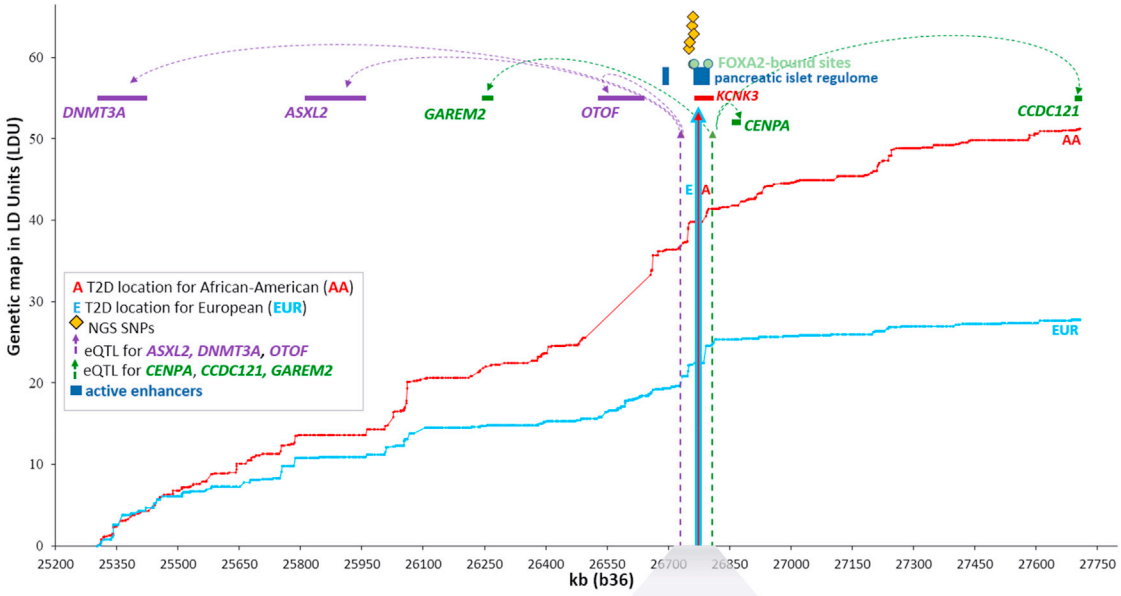

C

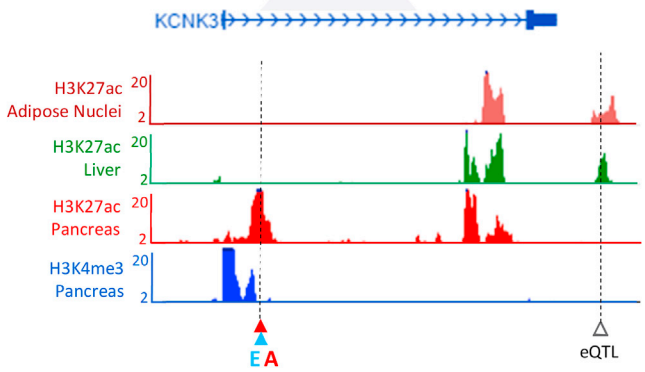

Figure 3. Candidate Causal Variants at T2D Locations in the *KCNK3* Region and Their Regulatory Role
(A) Identified T2D-associated SNPs using targeted next generation sequencing (NGS) of the functional location estimates on the LDU genetic maps and their risk allele frequency (RAF) in Europeans (EUR), African Americans (AA), East Asian (EAS), South Asian (SAS), and Mexican Americans (AMR).
(B) The two LDU genetic maps (y axis in LDU) for AA and EUR are plotted against the physical genomic region (x axis in kb). Vertical solid arrows represent the functional location estimates A and E that are associated with T2D in AA and EUR samples, respectively. The dotted arrows are the locations of eQTLs.
(C) −log10 p values of cell type-specific chromatin profiles are plotted against the kb map. T2D and eQTL locations overlap with the co-ordinates of the chromatin peaks.

cell types (Figure 3C), suggesting evidence for more than one functional mutation within this region. The full interval for the T2D and eQTL locations were not entirely covered by NGS data, but nevertheless, the associated NGS SNPs reside between two active islet enhancers (Figure 3B). In contrast to imputation methods that use high-resolution "out-of-sample" marker panels to infer missing SNPs to subsequently test one at a time, LDU analysis uses marker panels to infer high-resolution genetic maps. Subsequently, multi-marker tests of association use genetic distances for SNP arrays placed on those maps to infer the location of disease-associated functional variants. Fine mapping is therefore achieved by inferring fine-scale genetic maps, not by imputing SNPs. It is worth noting in relation to this that using the *KCNK3* locus as an example, the NGS SNPs genotyped for the case control data that were associated with T2D status (Figure 3A) could not be imputed based on the 1000G data as the reference panel.

A

		Allele		Summary statistics			RAF in other human populations				
NGS SNPs	kb (B36)	risk	other	OR	*P*	RAF	EUR	AA	EAS	SAS	AMR
rs7080591	114731	T	C	2.61	2.8E-04	0.746	0.615	0.549	0.678	0.591	0.503
rs7081062	114731	A	G	2.04	1.6E-03	0.755	0.643	0.639	0.694	0.640	0.530
rs10128255	114733	A	G	2.00	2.3E-03	0.755	0.643	0.639	0.695	0.640	0.530
rs4073980	114737	G	C	1.73	8.9E-03	0.609	0.498	0.779	0.049	0.376	0.339
rs4074718	114739	A	G	1.73	8.9E-03	0.609	0.499	0.779	0.050	0.377	0.337

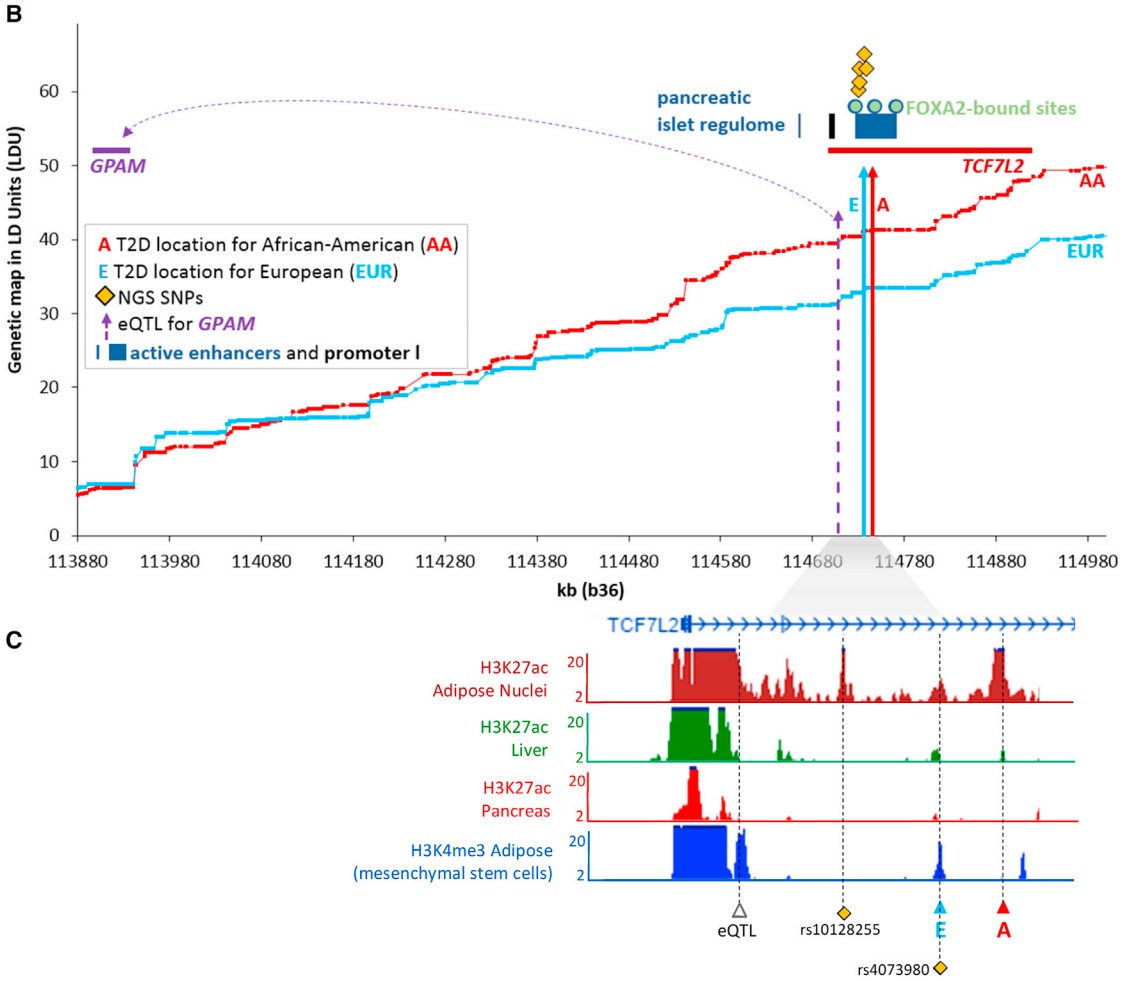

Figure 4. Candidate Causal Variants at T2D Locations in the *TCF7L2* Region and Their Regulatory Role

(A) Identified T2D-associated SNPs using targeted next generation sequencing (NGS) of the functional location estimates on the LDU genetic maps and their risk allele frequency (RAF) in Europeans (EUR), African Americans (AA), East Asian (EAS), South Asian (SAS), and Mexican Americans (AMR).

(B) The two LDU genetic maps (y axis in LDU) for AA and EUR are plotted against the physical genomic region (x axis in kb). Vertical solid arrows represent the functional location estimates A and E that are associated with T2D in AA and EUR samples, respectively. The dotted arrow is the location of eQTL.

(C) −log10 p values of cell type-specific chromatin profiles are plotted against the kb map. T2D, eQTL, and NGS SNP locations overlap with the co-ordinates of the chromatin peaks.

Findings at Previously Known T2D Loci

Using the same data and analytical methods, we have confirmed disease location estimates for 62 out of 76 previously known loci[3] (Table S1). Of these, about half (33/62) show evidence of being eQTL with the majority regulating *cis*-genes more than 1 Mb away. In addition, more than one-third (22/62) of the loci replicate for AA samples, which were previously excluded from trans-ethnic meta-analysis.[3] We investigated the Transcription factor 7-like 2 (*TCF7L2* [MIM: 602228]) locus (signal 117, Table S1). Figure 4B plots the T2D locations for EUR and AA and shows that this signal harbors a *cis*-eQTL for the distant *GPAM*. The T2D re-sequence variants we identified, which co-locate to the <30 kb interval between the T2D and eQTL locations, account for a large risk of disease (OR = 1.7–2.6). The summary statistics in Figure 4A show that these risk variants are the major allele in all other human populations. The T2D locations for both populations reside within an active enhancer cluster that is targeted by transcription factor FOXA2 (kb locations of the

regulatory elements are plotted on the x axis). Inferring the likely transcriptional activity by observing the chromatin state, we show that the eQTL, T2D co-locations, and NGS SNPs all map precisely to highly significant H3K4me3 and H3K27ac peaks, in particular in adipose cells (Figure 4C). This illustrates the importance of co-locating within an interval on the genetic map, since it allows for potential allelic heterogeneity.

Discussion

This study provides a comprehensive genomic catalog of susceptibility loci for T2D in European and African ancestry populations and evidence that the majority of the additional 111 and 62 previously known disease loci are eQTLs for 183 and 83 *cis*-genes, respectively. This implies that these disease loci confer risk of T2D via the *cis*-regulation of the expression levels in tissue relevant to T2D for a large number (266 in total) of neighboring genes. This study identifies a large number of disease loci at regulatory hotspots and replicates them in both European and African American populations, with 84% (93/111) of the additional loci being cosmopolitan. This replication was made possible by analyses that make use of, rather than being confounded by, the fine-scale differences in LD between these two populations, where causal locations and also eQTLs are estimated on an LDU map, avoiding the ambivalence of interpreting individual GWAS SNPs. Interestingly, recent results in the literature support our conclusion that cosmopolitan loci are more widespread than previously thought. For example, it was not until recently that the most established bona fide *TCF7L2* locus for T2D in Europeans was also confirmed in African ancestry groups in an extensive study that included 17 African American GWA samples.[7] This is a locus that was identified in the present study, which included only one African American sample.

The T2D-associated common genetic variation in *TCF7L2* is well established, but the mechanism by which risk of disease is conferred remains elusive. Our refined localization of this locus reveals that this is a regulatory site for the distant nuclear-encoded mitochondrial gene, *GPAM*, and identifies additional candidate causal variants. *GPAM* is interesting as it is a key rate-limiting enzyme in lipogenesis and highly expressed in liver and adipose tissue. Nuclear-encoded mitochondrial genes are of particular interest in relation to T2D, since mitochondrial function has been demonstrated to impact upon a myriad of molecular and cellular functional processes implicated in T2D.[24–26] However, to date human genetic association studies have identified few, if any, nuclear-encoded mitochondrial genes that directly confer risk of T2D in its common form. In this study we have identified at least 11 further nuclear-encoded mitochondria genes, which are regulated by eQTLs that also appear to confer risk of T2D. This indicates that one of the molecular mechanisms that contribute to inherited risk of T2D is mitochondrial dysfunction in relation to energy metabolism. These findings are also supported by an independent study design that utilizes transcriptome and proteome data to reconstruct metabolic pathways in myocytes and identify the same mitochondrial pathways implicated in our study for adipose tissue (namely, fatty acid beta-oxidation, Krebs cycle, pyruvate metabolism, and branched-chain amino acid [valine, leucine, and isoleucine] metabolism).[27]

Recent large-scale whole-genome and -exome association studies[28] have empirically questioned any major role for coding variants in the etiology of T2D and therefore make regulatory loci such as the ones highlighted in this study all the more important to investigate. We believe that the targeted re-sequencing of informative refined regions using case-control data has the power to dissect the genetic epidemiology of T2D. While imputation methods can successfully infer missing genotypes for most genomic regions using population data as the reference data, ironically it appears that imputation methods are likely to fail to impute or to make correct inferences where it matters most (e.g., at disease loci with allelic spectra that differ from the general population). This important point requires further investigation.

Chromatin analyses and targeted re-sequencing of these refined regions can be used to identify potential causal variant locations. The two identified signals (*ACTL7B* and *KCNK3*) that we have investigated lends support to this approach. A cosmopolitan disease location interval that includes *KCNK3* was observed to be a hotspot for the regulation of six neighboring genes, with *OTOF* of particular interest because of its known association with hearing loss (autosomal-recessive forms of deafness[29]). According to the NIDDK, the prevalence of low- or mid-frequency hearing impairment among diabetics is three times that of non-diabetics (28% compared with 9%)[30] with the potential mechanism operating via microvascular and neural damage due to long-term hyperglycemia.[31] Interestingly, adipose gene expression for *OTOF* has also been previously shown to be associated with BMI in the morbidly obese,[29] providing further evidence of a functional role through a regulatory mechanism. Targeted re-sequencing within the *KCNK3* location interval identified candidate causal variants with large effect sizes. As with the *TCF7L2* locus, the T2D and eQTL locations were found to reside in pancreatic islet enhancer and FOXA2 transcription factor-binding sites. Studies have shown that dysregulation of islet enhancers is relevant to the underlying mechanisms of T2D[22] and a recent examination of some of the previously found T2D loci have been found to overlap with FOXA2-bound sites.[32]

The cosmopolitan T2D location interval near *ACTL7B* overlapped with chromatin peaks for $CD14^+$ monocytes and included an eQTL for *KLF4* and *EPB41L4B*. *KLF4* is highly expressed in $CD14^+$ monocytes and belongs to the Krüppel-like factor (KLF) family that consists of transcription factors that can activate or repress different genes

involved in processes such as differentiation, development, and cell cycle progression, with several of these proteins implicated in glucose homeostasis.[33] Klf4 is also used experimentally to induce pluripotent cells that can differentiate into insulin-producing cells.[34] *EPB41L4B* codes for an erythrocyte membrane protein (EMP) with greatly increased EMP glycosylation observed in T2D-affected subjects[35] with likely clinical implications.[36] It is recognized clinically that both obesity and T2D are associated with a state of abnormal inflammatory response. Here we show that the T2D variants and eQTL locations for *KLF4* and *EPB41L4B* reside in regions with chromatin modifications mainly observed in $CD14^+$ monocytes. Monocytes play a pivotal role in innate immunity and are involved in metabolic regulation.[37] It has been shown that unbalanced proinflammatory/anti-inflammatory markers of $CD14^+$ cells is associated with metabolic disorder in obese T2D-affected individuals.[38] *KLF4* is a critical regulator of monocyte differentiation[39] and *EPB41L4B* expression in subcutaneous and omental adipose is strongly associated with BMI in morbidly obese individuals.[20] Therefore, these T2D intragenic variants and the regulated *cis*-genes (*KLF4* and *EPB41L4B*) are likely to be involved in an inflammatory pathway for obesity and T2D.

The complex causal chain between a gene and its effect on susceptibility cannot be unravelled until we have a full understanding of the regulatory genetic architecture that underpins T2D and until the causal changes have been localized in the DNA sequence.[40] Our results show that disease-associated loci in different populations, gene expression, and cell-specific regulatory annotation can be effectively integrated by localizing these effects on high-resolution linkage disequilibrium maps. By exploiting these maps to refine causal location estimates, we have identified a genomic catalog of cosmopolitan and European disease loci with correspondingly important clinical implications that provides important molecular insights and opportunities to understand the molecular basis of this devastating common disease.

Supplemental Data

Supplemental Data include two figures, two tables, and Supplemental Methods and can be found with this article online at http://dx.doi.org/10.1016/j.ajhg.2017.04.007.

Acknowledgments

We would like to thank the WTCCC, UK, for making the WTCCC T2D genomic data available. A full list of the investigators who contributed to the generation of the data is available from http://www.wtccc.org.uk. We are grateful to the NIDDK for making the AA T2D phenotype and genomic data available to us. The NIDDK whole-genome association search for T2D genes in African Americans was conducted by Donald Bowden, Center for Human Genomics, Center for Diabetes Research, Wake Forest University School of Medicine, with support from the NIDDK. The datasets used were obtained from the database of Genotypes and Phenotypes (dbGaP) at accession number phs000140. This manuscript was not prepared in collaboration with the labs of any of the investigators responsible for generating the data, and does not necessarily reflect the views or opinions of these investigators. T.A. would like to acknowledge the Medical Research Council UK (Investigator Award 91993) for supporting his work. All authors are grateful to Professor Dallas Swallow (UCL) for her valuable comments on the manuscript, Professor Philippe Froguel (Imperial College, CNRS 8199, EGID 59045) for generously supplying us with European DNA samples for the NGS pilot work, and Aminah Ali (UCL) for her valuable contributions to processing the NGS data. N.M. would like to acknowledge Newton E. Morton (University of Southampton) for the previous body of work on LDU maps.

Received: December 12, 2016
Accepted: April 11, 2017
Published: May 4, 2017

Web Resources

1000 Genomes, http://www.internationalgenome.org/
dbGaP, http://www.ncbi.nlm.nih.gov/gap
International HapMap Project, ftp://ftp.ncbi.nlm.nih.gov/hapmap/
Islet Regulome Browser, http://gattaca.imppc.org/isletregulome/home
OMIM, http://www.omim.org/
Roadmap, http://www.roadmapepigenomics.org/

References

1. Altshuler, D., and Daly, M. (2007). Guilt beyond a reasonable doubt. Nat. Genet. *39*, 813–815.
2. Lebovitz, H.E. (1999). Type 2 diabetes: an overview. Clin. Chem. *45*, 1339–1345.
3. Mahajan, A., Go, M.J., Zhang, W., Below, J.E., Gaulton, K.J., Ferreira, T., Horikoshi, M., Johnson, A.D., Ng, M.C., Prokopenko, I., et al.; DIAbetes Genetics Replication And Meta-analysis (DIAGRAM) Consortium; Asian Genetic Epidemiology Network Type 2 Diabetes (AGEN-T2D) Consortium; South Asian Type 2 Diabetes (SAT2D) Consortium; Mexican American Type 2 Diabetes (MAT2D) Consortium; and Type 2 Diabetes Genetic Exploration by Nex-generation sequencing in muylti-Ethnic Samples (T2D-GENES) Consortium (2014). Genome-wide trans-ancestry meta-analysis provides insight into the genetic architecture of type 2 diabetes susceptibility. Nat. Genet. *46*, 234–244.
4. Morris, A.P., Voight, B.F., Teslovich, T.M., Ferreira, T., Segrè, A.V., Steinthorsdottir, V., Strawbridge, R.J., Khan, H., Grallert, H., Mahajan, A., et al.; Wellcome Trust Case Control Consortium; Meta-Analyses of Glucose and Insulin-related traits Consortium (MAGIC) Investigators; Genetic Investigation of ANthropometric Traits (GIANT) Consortium; Asian Genetic Epidemiology Network–Type 2 Diabetes (AGEN-T2D) Consortium; South Asian Type 2 Diabetes (SAT2D) Consortium; and DIAbetes Genetics Replication And Meta-analysis (DIAGRAM) Consortium (2012). Large-scale association analysis provides insights into the genetic architecture and pathophysiology of type 2 diabetes. Nat. Genet. *44*, 981–990.
5. Li, Y.R., and Keating, B.J. (2014). Trans-ethnic genome-wide association studies: advantages and challenges of mapping in diverse populations. Genome Med. *6*, 91.

6. Asimit, J.L., Hatzikotoulas, K., McCarthy, M., Morris, A.P., and Zeggini, E. (2016). Trans-ethnic study design approaches for fine-mapping. Eur. J. Hum. Genet. *24*, 1330–1336.
7. Ng, M.C., Shriner, D., Chen, B.H., Li, J., Chen, W.M., Guo, X., Liu, J., Bielinski, S.J., Yanek, L.R., Nalls, M.A., et al.; FIND Consortium; eMERGE Consortium; DIAGRAM Consortium; MuTHER Consortium; and MEta-analysis of type 2 DIabetes in African Americans Consortium (2014). Meta-analysis of genome-wide association studies in African Americans provides insights into the genetic architecture of type 2 diabetes. PLoS Genet. *10*, e1004517.
8. Direk, K., Lau, W., Small, K.S., Maniatis, N., and Andrew, T. (2014). ABCC5 transporter is a novel type 2 diabetes susceptibility gene in European and African American populations. Ann. Hum. Genet. *78*, 333–344.
9. Elding, H., Lau, W., Swallow, D.M., and Maniatis, N. (2013). Refinement in localization and identification of gene regions associated with Crohn disease. Am. J. Hum. Genet. *92*, 107–113.
10. Zhang, X., Bailey, S.D., and Lupien, M. (2014). Laying a solid foundation for Manhattan–'setting the functional basis for the post-GWAS era'. Trends Genet. *30*, 140–149.
11. Wellcome Trust Case Control Consortium (2007). Genome-wide association study of 14,000 cases of seven common diseases and 3,000 shared controls. Nature *447*, 661–678.
12. Voight, B.F., Kang, H.M., Ding, J., Palmer, C.D., Sidore, C., Chines, P.S., Burtt, N.P., Fuchsberger, C., Li, Y., Erdmann, J., et al. (2012). The metabochip, a custom genotyping array for genetic studies of metabolic, cardiovascular, and anthropometric traits. PLoS Genet. *8*, e1002793.
13. Palmer, N.D., McDonough, C.W., Hicks, P.J., Roh, B.H., Wing, M.R., An, S.S., Hester, J.M., Cooke, J.N., Bostrom, M.A., Rudock, M.E., et al.; DIAGRAM Consortium; and MAGIC Investigators (2012). A genome-wide association search for type 2 diabetes genes in African Americans. PLoS ONE *7*, e29202.
14. Maniatis, N., Collins, A., and Morton, N.E. (2007). Effects of single SNPs, haplotypes, and whole-genome LD maps on accuracy of association mapping. Genet. Epidemiol. *31*, 179–188.
15. Maniatis, N., Collins, A., Gibson, J., Zhang, W., Tapper, W., and Morton, N.E. (2004). Positional cloning by linkage disequilibrium. Am. J. Hum. Genet. *74*, 846–855.
16. Maniatis, N., Collins, A., Xu, C.F., McCarthy, L.C., Hewett, D.R., Tapper, W., Ennis, S., Ke, X., and Morton, N.E. (2002). The first linkage disequilibrium (LD) maps: delineation of hot and cold blocks by diplotype analysis. Proc. Natl. Acad. Sci. USA *99*, 2228–2233.
17. Grundberg, E., Small, K.S., Hedman, A.K., Nica, A.C., Buil, A., Keildson, S., Bell, J.T., Yang, T.P., Meduri, E., Barrett, A., et al.; Multiple Tissue Human Expression Resource (MuTHER) Consortium (2012). Mapping cis- and trans-regulatory effects across multiple tissues in twins. Nat. Genet. *44*, 1084–1089.
18. Vionnet, N., Hani, E.H., Dupont, S., Gallina, S., Francke, S., Dotte, S., De Matos, F., Durand, E., Leprêtre, F., Lecoeur, C., et al. (2000). Genomewide search for type 2 diabetes-susceptibility genes in French whites: evidence for a novel susceptibility locus for early-onset diabetes on chromosome 3q27-qter and independent replication of a type 2-diabetes locus on chromosome 1q21-q24. Am. J. Hum. Genet. *67*, 1470–1480.
19. Meyre, D., Lecoeur, C., Delplanque, J., Francke, S., Vatin, V., Durand, E., Weill, J., Dina, C., and Froguel, P. (2004). A genome-wide scan for childhood obesity-associated traits in French families shows significant linkage on chromosome 6q22.31-q23.2. Diabetes *53*, 803–811.
20. Greenawalt, D.M., Dobrin, R., Chudin, E., Hatoum, I.J., Suver, C., Beaulaurier, J., Zhang, B., Castro, V., Zhu, J., Sieberts, S.K., et al. (2011). A survey of the genetics of stomach, liver, and adipose gene expression from a morbidly obese cohort. Genome Res. *21*, 1008–1016.
21. Consortium, E.P.; and ENCODE Project Consortium (2011). A user's guide to the encyclopedia of DNA elements (ENCODE). PLoS Biol. *9*, e1001046.
22. Pasquali, L., Gaulton, K.J., Rodríguez-Seguí, S.A., Mularoni, L., Miguel-Escalada, I., Akerman, I., Tena, J.J., Morán, I., Gómez-Marín, C., van de Bunt, M., et al. (2014). Pancreatic islet enhancer clusters enriched in type 2 diabetes risk-associated variants. Nat. Genet. *46*, 136–143.
23. Trynka, G., Sandor, C., Han, B., Xu, H., Stranger, B.E., Liu, X.S., and Raychaudhuri, S. (2013). Chromatin marks identify critical cell types for fine mapping complex trait variants. Nat. Genet. *45*, 124–130.
24. Lowell, B.B., and Shulman, G.I. (2005). Mitochondrial dysfunction and type 2 diabetes. Science *307*, 384–387.
25. Mootha, V.K., Lindgren, C.M., Eriksson, K.F., Subramanian, A., Sihag, S., Lehar, J., Puigserver, P., Carlsson, E., Ridderstråle, M., Laurila, E., et al. (2003). PGC-1alpha-responsive genes involved in oxidative phosphorylation are coordinately downregulated in human diabetes. Nat. Genet. *34*, 267–273.
26. Patti, M.E., and Corvera, S. (2010). The role of mitochondria in the pathogenesis of type 2 diabetes. Endocr. Rev. *31*, 364–395.
27. Väremo, L., Scheele, C., Broholm, C., Mardinoglu, A., Kampf, C., Asplund, A., Nookaew, I., Uhlén, M., Pedersen, B.K., and Nielsen, J. (2015). Proteome- and transcriptome-driven reconstruction of the human myocyte metabolic network and its use for identification of markers for diabetes. Cell Rep. *11*, 921–933.
28. Fuchsberger, C., Flannick, J., Teslovich, T.M., Mahajan, A., Agarwala, V., Gaulton, K.J., Ma, C., Fontanillas, P., Moutsianas, L., McCarthy, D.J., et al. (2016). The genetic architecture of type 2 diabetes. Nature *536*, 41–47.
29. Duman, D., and Tekin, M. (2012). Autosomal recessive nonsyndromic deafness genes: a review. Front. Biosci. (Landmark Ed.) *17*, 2213–2236.
30. Bainbridge, K.E., Hoffman, H.J., and Cowie, C.C. (2008). Diabetes and hearing impairment in the United States: audiometric evidence from the National Health and Nutrition Examination Survey, 1999 to 2004. Ann. Intern. Med. *149*, 1–10.
31. Bainbridge, K.E., Cheng, Y.J., and Cowie, C.C. (2010). Potential mediators of diabetes-related hearing impairment in the U.S. population: National Health and Nutrition Examination Survey 1999-2004. Diabetes Care *33*, 811–816.
32. Gaulton, K.J., Ferreira, T., Lee, Y., Raimondo, A., Mägi, R., Reschen, M.E., Mahajan, A., Locke, A., Rayner, N.W., Robertson, N., et al.; DIAbetes Genetics Replication And Meta-analysis (DIAGRAM) Consortium (2015). Genetic fine mapping and genomic annotation defines causal mechanisms at type 2 diabetes susceptibility loci. Nat. Genet. *47*, 1415–1425.
33. Gray, S., Feinberg, M.W., Hull, S., Kuo, C.T., Watanabe, M., Sen-Banerjee, S., DePina, A., Haspel, R., and Jain, M.K. (2002). The Krüppel-like factor KLF15 regulates the insulin-sensitive glucose transporter GLUT4. J. Biol. Chem. *277*, 34322–34328.
34. Noguchi, H. (2009). Recent advances in stem cell research for the treatment of diabetes. World J. Stem Cells *1*, 36–42.

35. Yamaguchi, M., Nakamura, N., Nakano, K., Kitagawa, Y., Shigeta, H., Hasegawa, G., Ienaga, K., Nakamura, K., Nakazawa, Y., Fukui, I., et al. (1998). Immunochemical quantification of crossline as a fluorescent advanced glycation endproduct in erythrocyte membrane proteins from diabetic patients with or without retinopathy. Diabet. Med. *15*, 458–462.
36. Adewoye, E.O., Akinlade, K.S., and Olorunsogo, O.O. (2001). Erythrocyte membrane protein alteration in diabetics. East Afr. Med. J. *78*, 438–440.
37. Fernández-Real, J.M., and Pickup, J.C. (2008). Innate immunity, insulin resistance and type 2 diabetes. Trends Endocrinol. Metab. *19*, 10–16.
38. Satoh, N., Shimatsu, A., Himeno, A., Sasaki, Y., Yamakage, H., Yamada, K., Suganami, T., and Ogawa, Y. (2010). Unbalanced M1/M2 phenotype of peripheral blood monocytes in obese diabetic patients: effect of pioglitazone. Diabetes Care *33*, e7.
39. Feinberg, M.W., Wara, A.K., Cao, Z., Lebedeva, M.A., Rosenbauer, F., Iwasaki, H., Hirai, H., Katz, J.P., Haspel, R.L., Gray, S., et al. (2007). The Kruppel-like factor KLF4 is a critical regulator of monocyte differentiation. EMBO J. *26*, 4138–4148.
40. Morton, N.E. (2005). Linkage disequilibrium maps and association mapping. J. Clin. Invest. *115*, 1425–1430.